CHAPTER I

OPTICAL PROPERTIES OF A COMPENSATED CHOLESTERIC MIXTURE: NON-ABSORBING CASE

1. Introduction

The optical behaviour of mixtures of right-handed and left-handed cholesteric liquid crystals (compensated cholesteric mixtures) has been the subject matter of many investigations. Friedel (1922) showed that that such a mixture results in a cholesteric structure whose pitch is sensitive to temperature and composition. For a given composition there is a temperature T_N at which the optical rotation is zero and the structure becomes a nematic (infinite pitch); on either side of T_N the rotations are of opposite signs indicating that the structure changes handedness on crossing this temperature. Recently, Sackmann et al. (1968) have directly determined the pitch as a function of temperature in a 1.75:1 weight mixture of cholesteryl chloride and cholesteryl myristate (CM) using laser diffraction techniques. They found that on increasing the temperature, the pitch of the sample gradually increased, becoming infinity at 42.5°C and then decreased with further increase of temperature. Their results are shown in Figure 1. Adams et al. (1970)

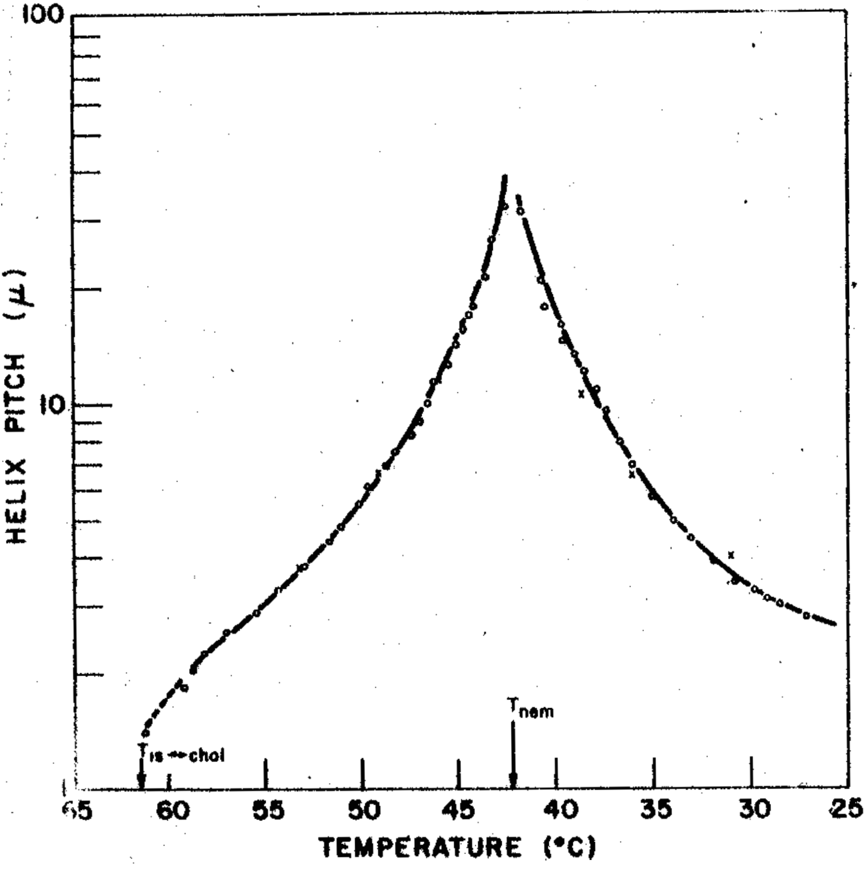

Figure 1: Temperature dependence of the pitch of a 1.75:1 mixture of cholesteryl chloride and cholesteryl myristate. The experimental data are taken from Sackmann et al. 1968 (see Baessler et al. 1969).

measured the variation of pitch as a function of composition of a cholesteryl chloride-cholesteryl nonanoate system at room temperature using the dispersive reflection technique. Their experiments indicated that in a compensated mixture the pitch depends on the composition in a way similar to the dependence of pitch on temperature, i.e., the pitch of the sample increases with increase in concentration of cholesteryl chloride, attains an infinite value for a particular concentration and then decreases with additional increase of cholesteryl chloride. The optical rotatory power in a 1.75:1 by weight CM mixture was measured as a function of temperature by Baeesler et al. (1969), for two specimens of thickness 3 µm and 10 pm. Their results are presented in figure 2. It can be seen that at any particular temperature the optical rotatory power ρ is not the same for the two samples, the difference being far more marked around T_N. Teucher <u>et al.</u> (1971) have determined the rotatory dispersion for various temperatures in a 1.75:1 by weight CM mixture. Their studies show that the change in the sign of ρ at T_N is due to the change in the helical sense of the system and that the system is right handed above T_N and left handed below T_N.

Figure 2: Rotatory power of a 1.75:1 mixture of cholesteryl chloride and cholesteryl myristate. (1) 10 µm sample, (2) 3 µm sample. (The dotted line indicates photomultiplier current at extinction position of polariser and analyser.) (Baessler *et al.* 1569).

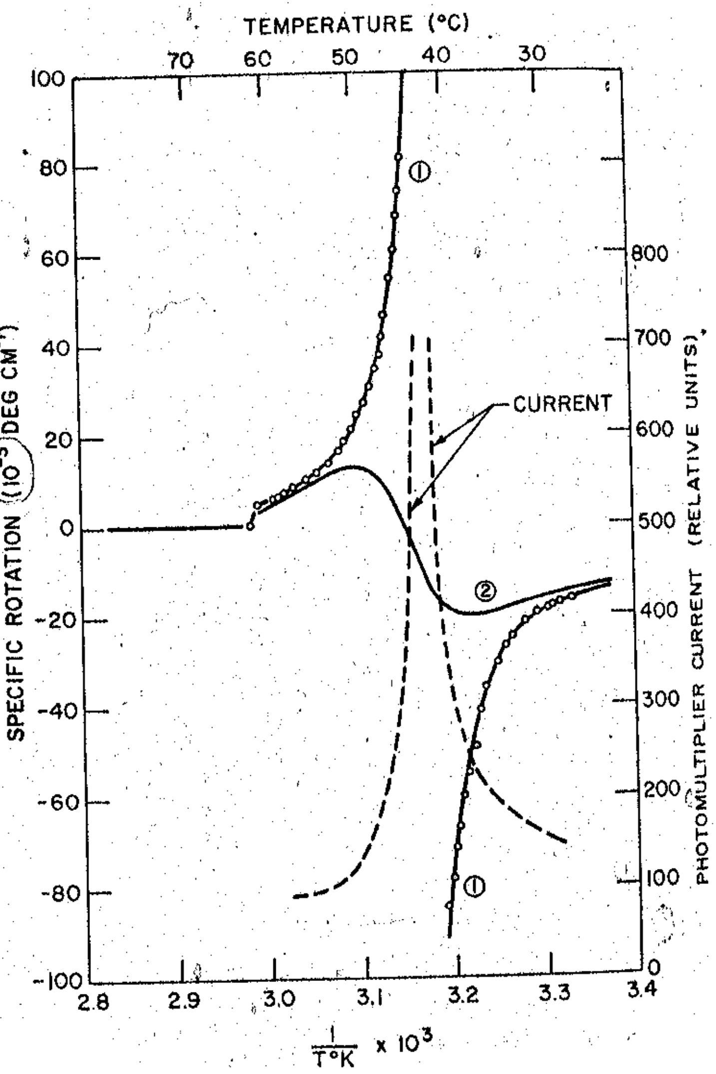
TEMPERATURE (°C)
70
60
50
40
30
100
80
60
40
20
0
-20
-40
-60
-80
-100
SPECIFIC ROTATION (10⁻³) DEG CM⁻¹)
800
700
600
500
400
300
200
100
0
PHOTOMULTIPLIER CURRENT (RELATIVE UNITS)
CURRENT
①
②
①
2.8
2.9
3.0
3.1
3.2
3.3
3.4
1/T°K x 10³

The previous workers have discussed their results on the basis of the de Vries equation (de Vries 1951),

$$\rho = -\frac{2\pi}{P}\,\frac{\alpha^2}{8\lambda'^2(1-\lambda'^2)} \qquad (1a)$$

where P is the pitch of the helix, $\alpha = \frac{\varepsilon_1 - \varepsilon_2}{2\varepsilon}$, ε_1 and ε_2 are the principal dielectric constants of the untwisted structure, $\varepsilon = \frac{1}{2}(\varepsilon_1 + \varepsilon_2)$, $\lambda' = \frac{\lambda}{P\varepsilon^{\frac{1}{2}}}$ and λ is the wavelength in vacuum.

This equation predicts infinite optical rotation at T_N whereas experiments indicate zero rotation at T_N. Furthermore, according to (1a), ρ should be independent of sample thickness, whereas the results of Baessler <u>et al</u>. (1969) show that this is not the case.

In view of these discrepancies, detailed experimental studies of the optical rotatory power of a compensated mixture as a function of temperature/pitch for various sample thicknesses were undertaken. The results are presented in this chapter. It is shown that the de Vries equation is not valid at temperatures close to T_N. The results are interpreted in terms of a rigorous theory developed by Chandrasekhar _et al._ (1973), Kini (1977). A brief summary of this theory is also presented.

2. Experiments

The measurements were made on a mixture of cholesteryl chloride and cholesteryl myristate taken in the ratio of 1.6:1 by weight. (Cholesteryl chloride was prepared in the Laboratory and cholesteryl myristate was obtained from Vari-Light Corporation, USA).

The transition temperatures of tho compounds used are given below.

Cholesteryl chloride:

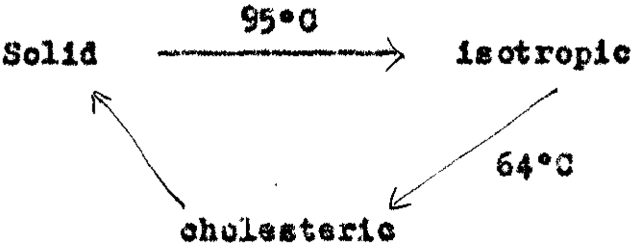

Cholesteryl myristate:

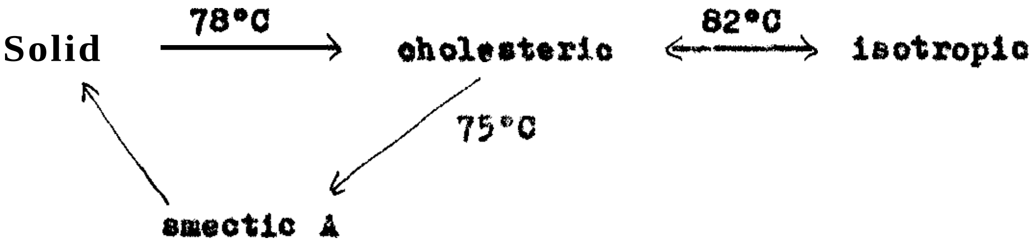

About 200-300 milligrams of the mixture was prepared in a small glass cup and it was heated in a oven to temperatures slightly above the cholesteric–isotropic transition temperature. It was stirred well with a glass rod to get homogeneous melt and then cooled to get the cholesteric phase,

The temperature of the sample was controlled by means of a specially constructed electric heater. It consisted of a copper tube of length 4.2 cm inner diameter 25 cm and outer diameter 5 cm. Around this tube, resistance wires were wound using mica sheets as insulator and the whole system was finally enclosed in a second copper tube. Glass windows were fixed on both sides of this outer tube to prevent air currents. Thermocouple wires contained in a ceramic capillary tube were introduced inside the heater through a small hole drilled in the copper tube. By controlling the current in the resistance wire it was possible to heat the system to any desired level. The temperature control was better than ± 0.1°C.

A copper–constantan thermocouple was used to measure the sample temperature. Its thermo e.m.f., measured with a vernier potentiometer and a spot deflection galvanometer system, was calibrated against a standard thermometer (Franz Küstner Nachf. KG., Dresden, G.D.R.). With this, the temperature could be measured to an accuracy of 0.05°C. The optical rotation was measured by means of a Winkel-Zeiss (Göttingen model No. 103071) polarimeter modified slightly to accommodate the complete heater assembly. The polarimeter consists of a Laurent's half shade and an analysing nicol mounted on a graduated disc. The rotation could be measured to an accuracy of 0.01°. The light source was a sodium lamp and all measurements were carried out at the wavelength 0.5893 µm.

Two identical glass discs (diameter 15 mm and thickness 2 mm) whose worked surfaces were flat to an order of λ/2 were used to contain the sample. Measurements were made for three sample thicknesses, viz., 12.7, 6.4 and 3 µm. Samples of 12.7 and 6.4 µm were obtained by using Dupont mylar spacers of thickness 0.5 and 0.25 mil respectively. [Here it was assumed that, the sample thickness is equal to the nominal spacer thickness, though in practice the sample thickness is often slightly higher due to edge, effects.] The 3 µm sample was prepared without using any spacer and the thickness was measured by forming interference fringes in the air spacer around the specimen. Since the plates could not be held perfectly parallel without a spacer, the thickness measurement of the 3 μm sample is estimated to be uncertain to ±25%.

The following procedure was adopted to get aligned samples: The substrates were thoroughly cleaned, successively with tsepol (wetting agent), concentrated NaOH, chromic acid, calcium carbonate and distilled water and then dried. The mixture heated to the cholesteric phase was sandwiched between the glass plates. Looking under a polarizing microscope one plate war displaced with respect to the other to and fro to get a well aligned plane textured sample. The entire cleaning process had to be repeated in cases where sample showed striations or domains. An aligned sample retained alignment more or Less to the same extent at all temperatures in the cholesterio phase except in the vicinity of T_N. At temperatures in the neighbourhood of T_N the sample developed inhomogeneities and at T_N it usually consisted of small domains. The degree of misalignment at T_N increased with increase in sample thickness. Also at T_N, it was not possible to completely cross the light transmitted by the sample. This may be due to the depolarization of the incident light.

The optical rotation measurements were made on cooling from the isotropic phase. For reasons pointed out above the measurement of ρ was comparatively difficult and less accurate very close to T_N. This was particularly so in thick specimens where ρ changes from a large positive value to a large negative value in a very small temperature interval around T_N. Therefore unless the temperature is kept truly constant, measurements become practically impossible. It was possible to determine in the region between the positive and negative peaks for the 3 µm sample and to a lesser degree of accuracy for the 6.4 µm sample but not for the 12.7 µm sample. The experimental values of ρ as a function of temperature (pitch) are given in figure 3. As the temperature is decreased, ρ increases initially, reaches a maximum, then starts decreasing and falls to zero at T_N. With further decrease of temperature ρ changes sign, increases in magnitude, reaching a second maximum and from then on gradually decreases. The interesting result obtained was that both the positions and magnitudes of the peak values of ρ are functions of the sample thickness.

Figure 3: Experimental rotatory power as a function of temperature for a 1.6 : 1 by weight mixture of cholesteryl chloride and oholeeteryl myristate. Sample thickness (a) 3 ± 0.75 μm, (b) 6.4 μm, (c) 12.7 μm.

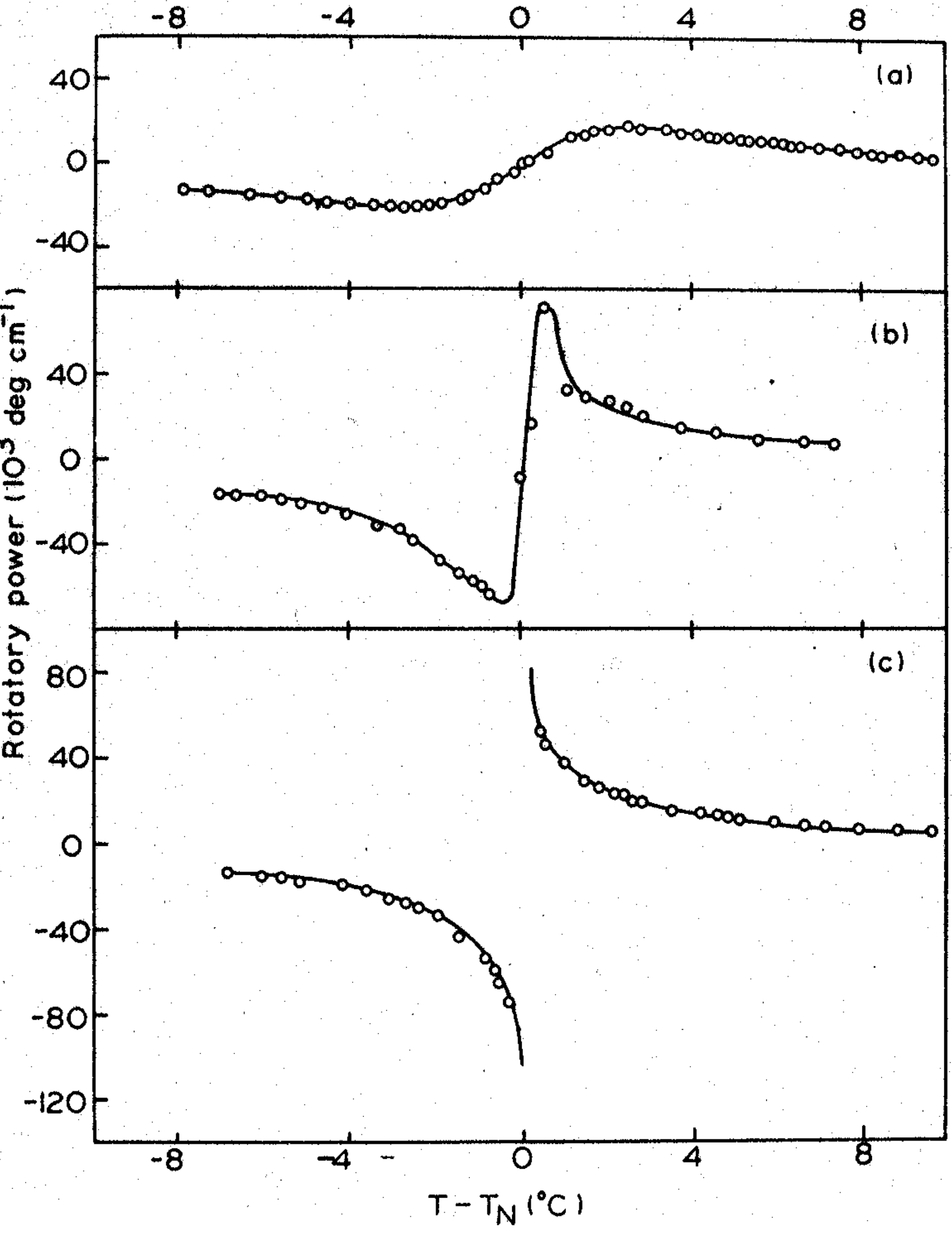
-8
-4
0
4
8
(a)
40
0
-40
(b)
40
0
-40
(c)
80
40
0
-40
-80
-120
Rotatory power (10^3 deg cm^{-1})
-8
-4
0
4
8
T – T$_N$ (°C)

The measurements show that the peak values increase in magnitude and move closer to T_N with increase in sample thickness, and that ρ is zero at T_N. This is very clear for the 3 µm and 6.4 µm samples but could not be established for the 12.7 µm sample due to experimental difficulties mentioned earlier.

The fact that ρ is dependent on sample thickness, especially in the neighbourhood of T_N and also that ρ vanishes at T_N establishes conclusively that equation (1a) is not valid, particularly close to T_N. We shall discuss the interpretation of these results on the basis of the rigorous theory.

3. Theory

Kini (1977) has derived an exact expression for ρ of a compensated mixture applying the Jones calculus (1941). This theory is reviewed here briefly.

The structure is regarded as a helically arranged pile of thin birefringent layers with the principal axes of the successive layers turned through a small angle β. The pitch P is assumed to be greater than λ, the wavelength of light in vacuum so that the effect of reflections is neglected completely.

Let light be incident normal to the layers, i.e., along; OZ. The principal axes of the first layer are assumed to be at an angle β with respect to the coordinate axes OX, OY. The Jones retardation matrix with respect to the principal axes is written as

$$G = \begin{bmatrix} e^{-i\gamma} & 0 \\ 0 & e^{i\gamma} \end{bmatrix}$$

where $\gamma = \frac{A}{\lambda}(\Delta\mu)p$ represents half the phase retardation produced by a single layer, $\Delta\mu = \mu_1 - \mu_2$ is the layer birefringence and p is the layer thickness.

With respect to OX, OY this retardation matrix is

$$J_1 = SGS'$$

where

$$S = \begin{bmatrix} \cos\beta & -\sin\beta \\ \sin\beta & \cos\beta \end{bmatrix}$$

and $S' = S^{-1}$ is the transpose of S, so that $SS' = S'S = E$, the unit matrix.

The retardation matrix for 'n' layers is

$$J_n = S^n(GS')^n = \begin{bmatrix} a & b \\ c & d \end{bmatrix}, \qquad (1b)$$

It can be shown that

$$(GS')^n = \frac{\sin n\theta}{\sin\theta}(GS') - \frac{\sin (n-1)\theta}{\sin\theta}\begin{bmatrix} 1 & 0 \\ 0 & 1 \end{bmatrix} \qquad (2)$$

where $\cos\theta = \cos\beta \cos\gamma$.

since β and γ are small [$\beta = \frac{2\pi}{P}b$. Taking $b = 10x10^{-8}$ cm and $P = 5x10^{-4}$ cm, $\beta \sim 10^{-3}$]

$$\theta^2 \simeq \beta^2 + \gamma^2 \qquad (3)$$

From (1b) and (2)

$$a = [\cos n\beta \cos n\theta + \frac{\tan\beta}{\tan\theta}\sin n\beta \sin n\theta]$$

$$- i[\frac{\sin n\theta}{\sin\theta}\sin\gamma \cos(n+1)\beta] \qquad (4)$$

$$b = [\frac{\tan\beta}{\tan\theta}\cos n\beta \sin n\theta - \sin n\beta \cos n\theta]$$

$$- i[\frac{\sin n\theta}{\sin\theta}\sin\gamma \sin(n+1)\beta] \qquad (5a)$$

$$c = -b^*, \quad d = a^*, \quad i = (-1)^{\frac{1}{2}}$$

where a^* and b^* are respectively the complex conjugates of a and b.

A system of the above type can be treated as a rotator and a retarder. If ρ_t is the total rotation produced by the system, 2φ the phase retardation and ψ the azimuth of the principal axes of the retarder,

$$J_n = \begin{bmatrix} \cos\rho_t & -\sin\rho_t \\ \sin\rho_t & \cos\rho_t \end{bmatrix} \begin{bmatrix} \cos\psi & -\sin\psi \\ \sin\psi & \cos\psi \end{bmatrix}$$

$$\times \begin{bmatrix} \exp -i\varphi & 0 \\ 0 & \exp i\varphi \end{bmatrix} \begin{bmatrix} \cos\psi & \sin\psi \\ -\sin\psi & \cos\psi \end{bmatrix} \qquad (5b)$$

From (1b) and (5b)

$$a = \cos\varphi\cos\rho_t - i\sin\varphi\cos(2\psi + \rho_t) \qquad (6)$$

$$b = -\cos\varphi\sin\rho_t - i\sin\varphi\sin(2\psi + \rho_t) \qquad (7)$$

$$c = -b^* \quad \text{and} \quad d = a^* .$$

Equating real and imaginary parts of (4) and (6), and (5a) and (7), one gets

$$\rho_t = n(\beta - \theta') \text{ radians} \qquad (8)$$

$$\varphi = \cos^{-1}\left[\frac{1 + \tan^2 n\theta'}{1 + \tan^2 n\theta}\right]^{\frac{1}{2}} \qquad (9)$$

$$\psi = \tfrac{1}{2}[(n + 1)\beta - \rho_t]$$

where

$$\theta' = \frac{1}{n} \tan^{-1} \left[\frac{\tan \beta \; \tan n\theta}{\tan \theta}\right] \qquad (10)$$

Equation (8) represents optical rotation for n layers, that is for a sample thickness np.

The optical rotatory power is given by

$$\rho = \frac{\rho t}{np} = \frac{1}{p}(\beta - \theta') \text{ radians} \qquad (11)$$

At temperatures well away from the nematic point T_N, the pitch is relatively small, β becomes much larger than γ, and from (3) and (10) $\theta' \simeq \theta$. The optical rotatory power then becomes

$$\rho \simeq \frac{1}{p}(\beta - \theta) = \frac{1}{p}[\beta - (\beta^2 + \gamma^2)^{\frac{1}{2}}]$$

$$= -\frac{1}{p} \; \frac{\gamma^2}{2\beta}$$

$$= -\frac{\pi^2(\Delta\mu)^2 p}{2\beta\lambda^2}$$

$$= -\frac{\pi(\Delta\mu)^2 p}{4\lambda^2} , \qquad (12)$$

which is the Mauguin-de Vries equation. As the temperature approaches T_N (i.e., for very high pitch values), ρ given by (11) departs from (1a) and (12). At $T = T_N$, $P = \infty$, $\theta' = \beta = 0$, and the rotation vanishes for all values of sample thickness, whereas (1a) and (12) predict infinite rotation.

Theoretical curves giving the dependence of the rotatory power on temperature of 1.75 : 1 CM mixture calculated using equation (11) are shown in Figure 4. The ρ values are calculated for $\lambda = 5893$ Å and layer thickness $b = 10$ Å. The dependence of pitch on temperature has been taken from the data of Sackmann *et al*. (1968) for the 1.75: 1 CM mixture. The layer birefringence $\Delta\mu$ at 20°C and 55°C were calculated by fitting the observed values (Baessler *et al*. 1969) of ρ in equation (12) at these, temperatures which are far away from T_N and the intermediate values were obtained by interpolating linearly.

The curves in Figure 4 show that with increasing sample thickness, the positive and negative peaks in the rotatory power increase in height and also get closer to T_N and thereby for thick samples the reversal in the sign of rotation takes place fairly abruptly. Comparing figures 3 with 4, it is clear that the trends in the observed data can be accounted for by this theory.

Figure 4: Theoretical variation of the rotatory power with temperature (and inverse pitch) for [1.75 : 1 CM (by weight) mixture] samples of thicknesses 2 µm, 6 µm and 10 µm. The broken curve is the rotatory power given by the Mauguin-de Vries equation.

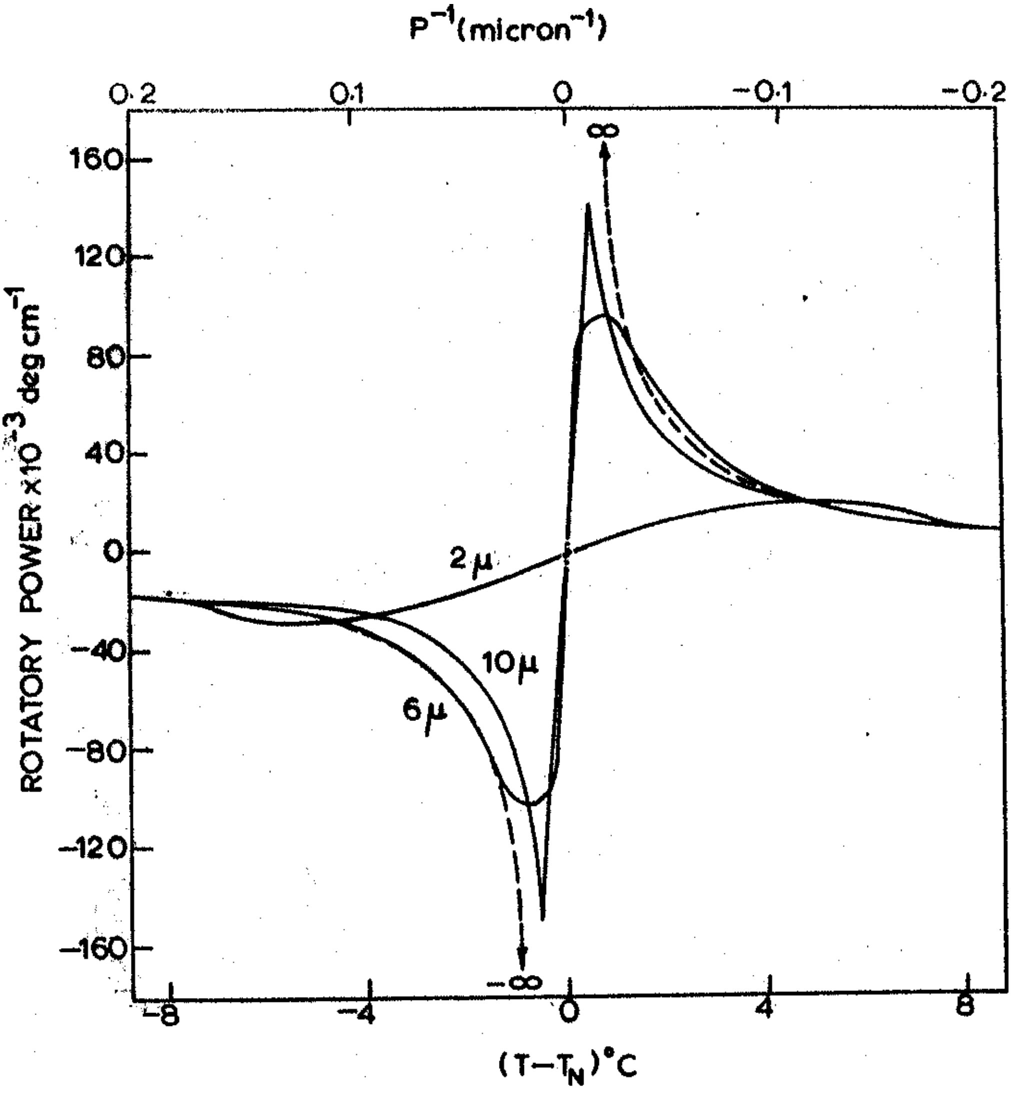
P^{-1}(micron^{-1})
0·2
0·1
0
−0·1
−0·2
ROTATORY POWER ×10^{-3} deg cm^{-1}
160
120
80
40
0
−40
−80
−120
−160
∞
−∞
2μ
10μ
6μ
−8
−4
0
4
8
(T−T$_N$)°C

References

Adams, J.E., Haas, W. and Wysocki, J.J. 1970 Liquid Crystals and Ordered Fluids, Eds. J.F.Johnson and R.S. Porter (Plenum Press), p.463.

Baessler, H., Laronge, T.M. and Labes, M.M. 1969 J.Chem.Phys. , 3213.

Chandrasekhar, S., Ranganath, G.S., Kini, U.D. and Suresh, K.A. 1973 Mol.Cryst.Liquid Cryst. **24**, 201.

de Vries, H. 1951 Acta Cryst. **4**, 219.

Friedel M.G. 1922 Ann. Phys. , 273.

Jones, R.C. 1941 J. Opt. Soc. Amer. **31**, 488.

Kini, U.D. 1977 Thesis, University of Mysore.

Mauguin, M.C. 1911 Bull. Soc. Franc. Miner. Crist. **34**, 71.

Sackmann, E., Meiboom, S., Snyder, L.C., Meixner, A.E. and Dietz, R.E. 1968 J.Amer.Chem.Soc. **90**, 3567.

Teucher, I., Ko, K. and Labes, M.M. 1972 J. Chem. Phys. **56**, 3308.

CHAPTER II

OPTICAL PROPERTIES OF A COMPENSATED CHOLESTERIC MIXTURE: ABSORBING CASE

1. Introduction

In the previous Chapter we presented some results on a non-absorbing compensated cholesteric mixture. In this Chapter we discuss the properties of an absorbing compensated mixture; in particular we investigate the circular dichroism of such a mixture. Saeva and Wysocki (1971) showed that the addition of a small quantity of linearly dichroic molecules in a non-absorbing cholesteric can give rise to circular dichroism in the region of the absorption band of the solute molecules. They dissolved a small quantity of n-(p-methoxybenzylidene)-p-n-butylaniline (MBBA) in a cholesteryl chloride-cholesteryl nonanoate system. Their circular dichroism spectra of the system for the cases of left-handed solvent and right-handed solvent as well as the absorption spectrum of MBBA are given in Figure 1. (In this thesis, we refer the circular dichroism due to solute molecules as 'induced circular dichroism' to distinguish

Figure 1

Circular dichroism (upper) and absorption spectrum (lower): - - - - - - -, 6.3 µm film containing 52.9 mg of MBBA in 10.0 g. of 27.7:72.3 weight per cent cholesteryl chloride and cholesteryl nonanoate (right hand helix); ————————, 11.7 µm film containing 63.19 mg of MBBA in 10.0 g. of 90.6:9.4 weight per cent cholesteryl chloride and cholesteryl nonanoate (left hand helix). The bands around 550 λ (µm) are due to Bragg reflection and those around 300 λ (µm) are due to the absorption by the solute molecules (Saeva and Wysocki 1971).

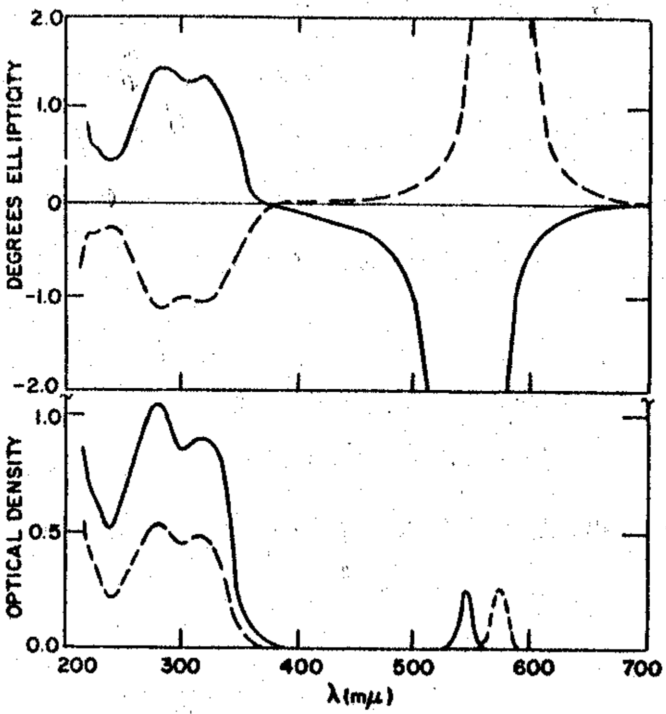
2.0
1.0
0
-1.0
-2.0
DEGREES ELLIPTICITY
1.0
0.5
0.0
OPTICAL DENSITY
200
300
400
500
600
700
λ(mμ)

it from the circular dichroism that occurs at the reflection band in a cholesteric.) They demonstrated that changing the handedness of the solvent changes the sign of the induced circular dichroism (ICD) and that when the cholesteric medium is converted to a nematic (either by using a compensated mixture at temperature T_N or by untwisting the cholesteric by the application of an electric field), the ICD reduces to zero indicating that a macroscopic helical structure is necessary for the induced effect and not just a chiral solvent.

Sackmann and Voss (1972), after studying ICD in several systems found that the sign of the ICD depends on the sign of the linear dichroism of the solute molecules. To interpret the origin of ICD in cholesterics, they assumed that the solute molecules adopt the same helical arrangement as the solvent molecules on a macroscopic scale. They also assumed that the solute molecules alone contribute to the absorption and linear dichroism of the cholesteric layers. Based on this model and the de Vries theory of light propagation in cholesterics, Sackmann and Voss theoretically calculated the ICD of cholesteric medium and showed that the predicted features are in qualitative agreement with the observations.

However, in the above cases, the experimental observations pertain only to the regime $\frac{\lambda}{\lambda_{max}} \gg \frac{\Delta\mu}{2\mu}$ i.e., $P \ll \lambda/\Delta\mu$ ($\lambda_{max} = P\mu$, μ = average refractive index). The theoretical treatment of Sackmann and Voss holds good in this regime. In the present Chapter, studies are described on ICD as a function of temperature/pitch in the regime $P \gg \lambda/\Delta\mu$ for different sample thicknesses. This has led to some interesting new observations that have so far been overlooked in previous studies.

2. Absorbing compensated cholesteric mixture

The sample was prepared by dissolving 1.48% by weight of β-carotene (Merck, Germany) in a 1.64:1 by weight cholesteryl chloride-cholesteryl myristate (CM) mixture. The dye β-carotene has a strong linear dichroic band around 0.48 μm. Figure 2 gives the polarised absorption spectra of β-carotene. The mixture taken in a small glass cup was heated in a oven to a temperature slightly above the cholesteric-isotropic transition temperature and stirred well to get a homogeneous melt, As the melt was cooled it

Figure 2: Spectra of 5×10^{-4} M β-carotene in a 1.9 : 1 by weight CM mixture (T_N = 40°C). The sample was aligned for 12 hr. in a magnetic field of strength 20 KG applied along the helical axis (T ≈ 35°C). In the upper spectrum the electric vector of the light is perpendicular, and in the lower spectrum parallel, to the magnetic field. The cholesteryl chloride and cholesteryl myristate molecules align perpendicular to the direction of the magnetic field (Sackmann 1968).

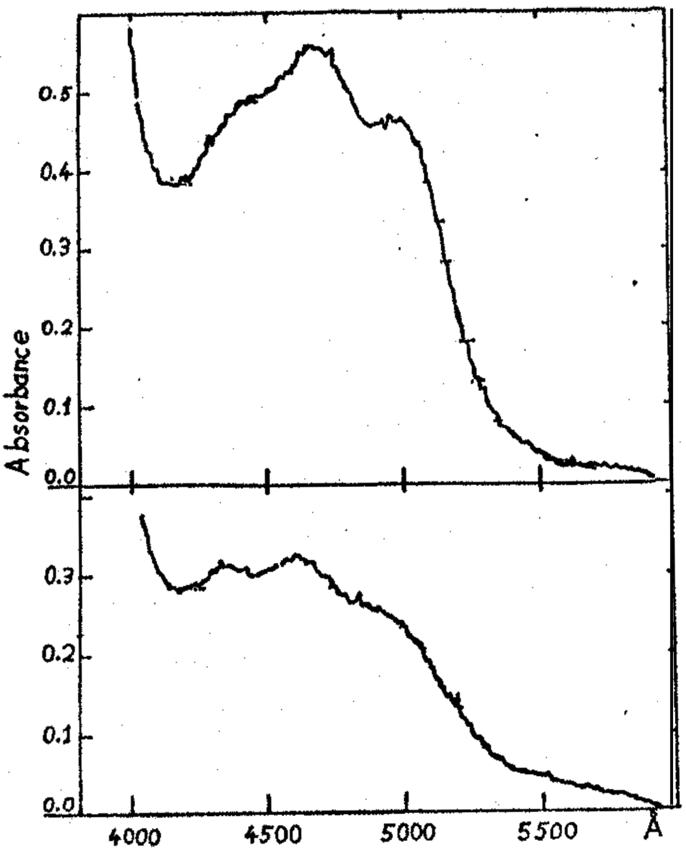
Absorbance
0.5
0.4
0.3
0.2
0.1
0.0
0.3
0.2
0.1
0.0
4000
4500
5000
5500
Å

adopted a cholesteric structure.

To vary and to control the temperature of the sample an electrical heater (described in Chapter I) was used. The temperature of the sample was sensed by a copper–constantan thermocouple. The procedure for the calibration of the thermocouple and the measurement of thermo e.m.f. was similar to that explained in Chapter I.

A block diagram of the experimental set up to measure CD is given in figure 3. The light source was a tungsten filament lamp with a short focus lens positioned to give a parallel beam. It was run on a highly stabilized power supply. To improve the signal to noise ratio, a chopper, lock–in–umplifier system was used. The chopper was a metal wheel with apertures and rotated by a motor, the rotation of which was adjusted to chop the light beam at 321 cycles/second. A Mekee Pederson reflection grating monochromator (Model MP 108, USA) was used to get 0.5 µm radiation at which these experiments were conducted. Circularly polarised light was obtained by means of a Winkel-Zeiss polarising microscope attachment; it consisted of a nicol prism that could

Figure 3: A block diagram of the experimental arrangement used to determine the circular dichroism.

1 Tungsten filament light source
2 Mechanical chopper
3 Detector for reference signal
4 Monochromator
5 Circular polariser
6 Sample chamber
7 Photomultiplier tube
8 High tension power supply
9 Lock-in-amplifier
10 Oscilloscope
11 Microvoltmeter
12 Stabilised power supply.

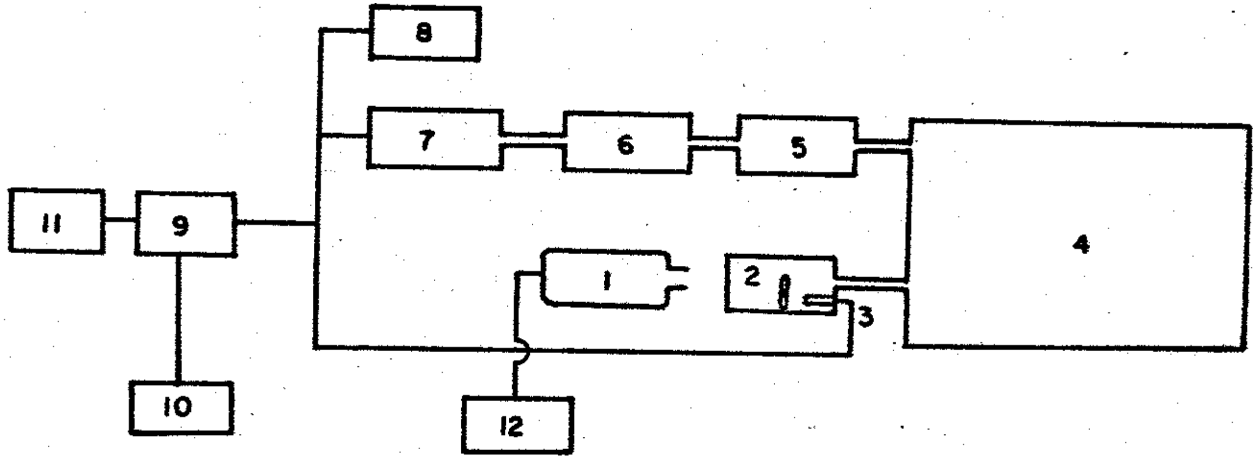
8
7
6
5
4
11
9
1
2
3
10
12

be set at two orthogonal positions and a quarter wave plate with principal axes inclined at 45° with respect to the nicol. Depending on the position of the nicol the emergent light was either left circular or right circular. To avoid stray light the heater assembly was placed in a chamber provided with suitable windows for making these measurements. The light transmitted by the sample was detected by a photo-multiplier (Model M10 FQS 29 Carl Zeiss, Zena). The signal was analysed by a lock-in-amplifier and the resulting signal was measured using a Philips D.C. microvoltmeter. (The lock-in-amplifier was constructed by Dr.S.R.Rajagopalan and Mr. A. Pujari of the Materials Science Division of National Aeronautical Laboratory, Bangalore and the measurements were carried out at their laboratory. I am grateful to them and to Dr.S.Ramaseshan, Head, Materials Science Division for extending the facilities and for helpful advice.)

The sample was sandwiched between two optically flat $(\sim\lambda/2)$ glass discs and the thickness of the sample was fixed using spacers. Measurements were made for five sample thicknesses 12.7, 9.5, 8, 6.3 and 4 μm. Standard Dupont mylar spacers of thickness 0.5 mil and 0.25 mil were used for the 12.7 and 6.4 μm film samples and mica spacers for 4, 8 and 9.5 μm samples. The uniformity in the thickness of the mica spacer was tested with a dial guage (Model MI/100 B Carl Zeiss, Zena). The thickness measurements of mica spacers were accurate to $\pm\frac{1}{2}$ μm. It was assumed that the sample thickness is equal to the spacer thickness. (It is known that the actual sample thickness may sometimes be slightly higher due to edge effects but no allowance wars made for this in the present study.)

Plane texture films were obtained by cover plate displacement method described in Chapter I. Before making the measurement of intensity, the alignment In the sample was checked using a polarizing micro-eooye. An aligned sample retained alignment approximately to the same degree at all temperatures except in the vicinity of T_N where it broke into small domains. The degree of misalignment at T_N increased with increase in sample thickness. The determination of circular dichroism in the cholesteric phase was started soon after cooling from the isotropic phase.

The transmitted intensities I_R and I_L were measured (as voltages in the DC microvoltmeter) for incident right- and left-circularly polarized light at every temperature and the circular dichroism wars expressed as

$$D = \frac{I_R - I_L}{I_R + I_L + 2(I_R I_L)^{\frac{1}{2}}}$$

The dichroic power $\mathcal{D}$ is given by

$$\mathcal{D} = \frac{D}{t}$$

where t = sample thickness. (It will be noted that this definition of D and $\mathcal{D}$ eliminates the necessity for expressing the intensities in absolute units.)

Away from T_N the error in the intensity measurements were less than 2%. But close to T_N this error increased slightly. Also the error in the intensity measurement in the neighbourhood of T_N increased with increasing sample thickness for reasons explained earlier.

3. Results

In figure 4 is given the experimental dependence of the dichroic power) on temperature for various sample thicknesses. For any sample thickness the behaviour of $\mathcal{D}$ versus temperature is analogous to that of the optical rotatory power in a non-absorbing compensated mixture (treated in Chapter I). At T_N $\mathcal{D}$ is equal to zero. It is negative on the lower temperature side and positive on the higher temperature

Figure 4: Experimental values of dichroic power versus temperature for different thicknesses of the sample in a 1.64 : 1 by weight mixture of cholesteryl chloride and cholesteryl myristate containing 1.48% by weight of β-carotene.

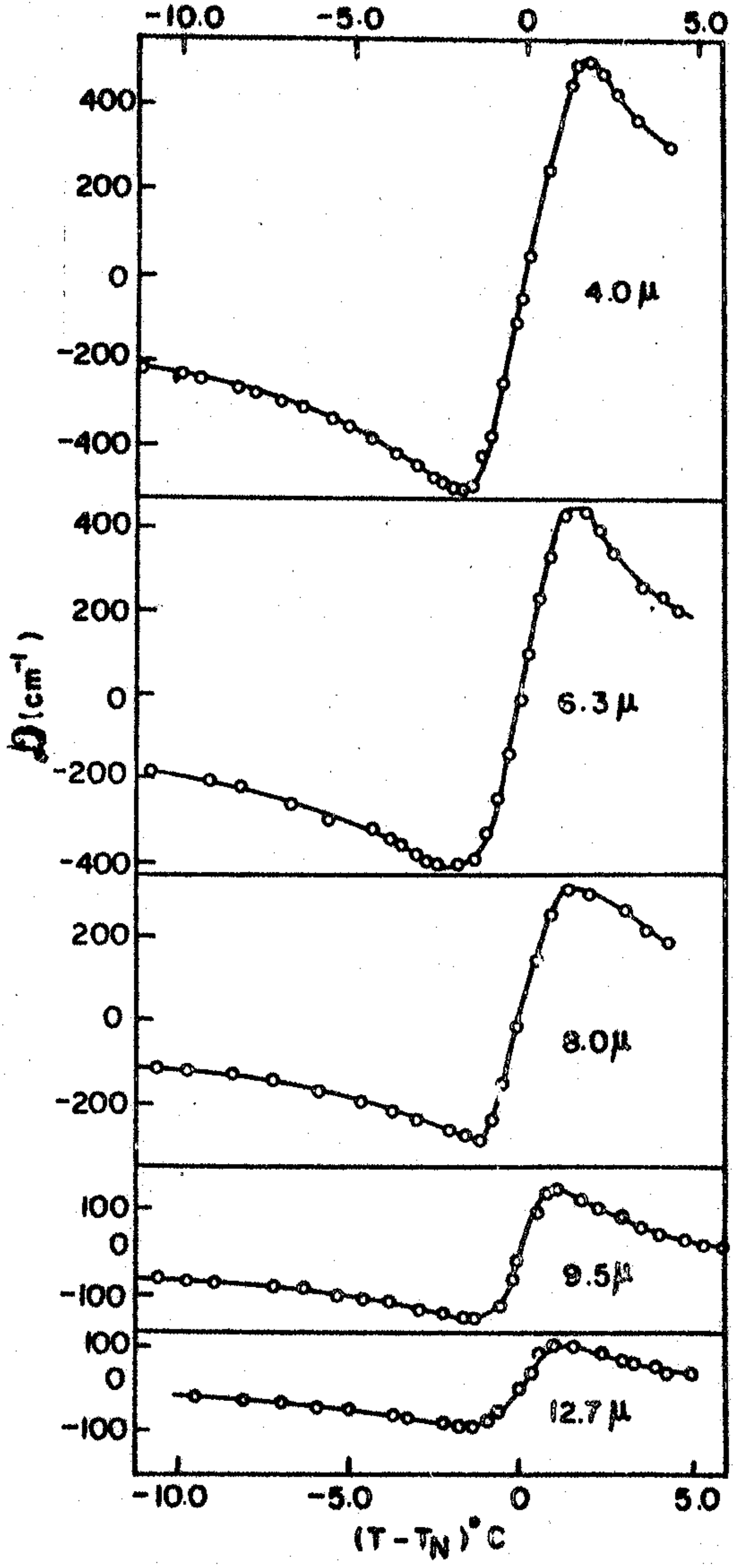

-10.0
-5.0
0
5.0
400
200
0
-200
-400
4.0 μ
400
200
0
-200
-400
6.3 μ
200
0
-200
8.0μ
100
0
-100
9.5μ
100
0
-100
12.7 μ
-10.0
-5.0
0
5.0
$(T - T_N)$ °C
$\mathcal{D}$ (cm^{-1})

side of T_N, the variation being almost symmetric about this temperature. $\mathcal{D}$ increases rapidly as one moves away (on either side) from T_N reaching a maximum at a characteristic temperature and then decreases gradually. The most interesting result from this figure is that the peak dichroic power <u>decreases</u> as the sample thickness increases in the range 4 to 12.7 μm. This behaviour is different from normal absorbing optically active materials which exhibit thickness independent circular dichroism. In addition, the position and the magnitudes of the peak values are functions of sample thickness, the peaks moving away from T_N and becoming less and less sharp with increase in sample thickness. We shall now discuss the interpretation of these results on the basis of the rigorous theory due to Kini (1977).

4. <u>Theory</u>

Sackmann and Voss (1972) who established that ICD is due to helical stacking of linearly dichroic molecules have treated this problem in two extreme cases:

1)

$$\frac{\lambda}{\lambda_{max}} \gg \frac{\Delta\mu}{2\mu} \quad \text{i.e.,} \quad P \ll \frac{\lambda}{\Delta\mu}$$

On this assumption they have obtained an expression for the aircular dichroism whiah satisfactorily explains their experimental observations.

2) $$\frac{\lambda}{\lambda_{max}} \ll \frac{\Delta\mu}{2\mu} \quad \text{i.e.,} \quad P \gg \frac{\lambda}{\Delta\mu}$$

This holds good for very large pitch values, i.e., in systems like the twisted nematic devices (obtained by rotating the walls containing a nematic) where the normal waves are linear vibrations polarised along and perpendicular to the local director. In compensated mixtures, however, pitch values in the range $P \gg \frac{\lambda}{\Delta\mu}$ also occur and at these pitch values the waves are elliptically polarised. Hence the treatment by Sackmann and Voss (1972) is not valid in this regime. The theory of optical rotatory power given in Chapter I has been extended by Kini (1977) to explain the optical properties of absorbing twisted structures.

As before the choleeteric structure is looked upon as a helical stack of very thin birefringent layers. Eaoh layer is supposed to have uniaxial symmetry with the principal axis of the successive layers turned through a small angle β. In addition to the phase retardation 2γ per layer, defined as $2\gamma = \frac{2\pi}{\lambda}(\Delta\mu)p$, one also has anisotropic absorption in the layers. The axes of the principal absorption coefficients k_1 and k_2 are assumed to coincide with the principal axes of the refractive indices μ_1 and μ_2. In this case, the Jones matrix of any layer with reference to its principal axes is

$$G_o = \begin{bmatrix} \exp(-i\gamma) & 0 \\ 0 & \exp(i\gamma) \end{bmatrix} \begin{bmatrix} \exp(-k_1 p) & 0 \\ 0 & \exp(-k_2 p) \end{bmatrix}$$

$$= \exp(-\alpha) \begin{bmatrix} \exp(-i\hat{\gamma}) & 0 \\ 0 & \exp(i\hat{\gamma}) \end{bmatrix} \qquad (1)$$

where

$$\alpha = \left(\frac{k_1 + k_2}{2}\right)p \quad \text{and} \quad \hat{\gamma} = \gamma - i\left(\frac{k_1 - k_2}{2}\right)p = \gamma - i\delta.$$

(Here the convention followed is that the phase factor at any point Z is given by $\exp[-i(2\pi\mu Z/\lambda)]$).

If the principal axes of the first layer be inclined at an angle β with respect to OX, OY of the coordinate system XYZ with light travelling along OZ, then the Jones matrix of the nth layer with respect to XY is

$$G_n = S^n G_o S^{-n} \qquad (2)$$

where

$$S^n = \begin{bmatrix} \cos n\beta & -\sin n\beta \\ \sin n\beta & \cos n\beta \end{bmatrix}$$

and S^n is the inverse of S^{-n} (i.e., $S^n S^{-n} = E$, the unit matrix). For n layers the, net Jones matrix is given by

$$J_n = G_n \cdot G_{n-1} \cdot G_{n-2} \ldots\ldots G_2 \cdot G_1$$

$$= S^n G_o S^{-n} S^{n-1} \cdot G_o S^{-(n-1)} \ldots\ldots S G_o S^{-1}$$

But $\quad S^m S^n = S^{m+n}$

Hence

$$J_n = S_n (G_o S^{-1})^n \qquad (3)$$

If λ_1 and λ_2 are the eigenvalues of $(G_o S^{-1})$ then one can show that

$$(G_oS^{-1})^n = \frac{\lambda_1^n - \lambda^n}{\lambda_1 - \lambda_2}(G_oS^{-1}) - \lambda_1\lambda_2\frac{\lambda_1^{n-1} - \lambda_2^{n-1}}{\lambda_1 - \lambda_2} E$$

where λ, and λ_2 are given by

$$\lambda_1 = \exp(-\alpha)\exp(i\hat{\theta}) \quad \text{and} \quad \lambda_2 = \exp(-\alpha)\exp(-i\hat{\theta})$$

with

$$\cos\hat{\theta} = \cos\hat{\gamma}\cos\beta$$

Therefore

$$(G_oS^{-1})^n = \exp(-n\alpha)\frac{\sin n\hat{\theta}}{\sin\hat{\theta}}(G_oS^{-1}) - \exp[-(n+1)\alpha]\frac{\sin(n-1)\hat{\theta}}{\sin\hat{\theta}}E$$

$$\simeq \exp(-n\alpha)\left[\frac{\sin n\hat{\theta}}{\sin\hat{\theta}}(G_oS^{-1}) - \frac{\sin(n-1)\hat{\theta}}{\sin\hat{\theta}}E\right] \qquad (4)$$

Since n is very large compared to unity.

Using (3) and (4) the net Jones matrix J_n can be worked in terms of β, γ, k_1, k_2 and n.

The matrix J_n can also be uniquely resolved into a rotator, a retarder, a circularly dichroic plate and a linearly dichroic plate. The unique matrix resolution is given by

$$J_n = \exp(-\chi)\Upsilon^{R}\Sigma\Phi\mathcal{K}\Sigma\Upsilon^{-1} \qquad (5)$$

where

$$\boldsymbol{\Psi} = \begin{bmatrix} \cos\psi & -\sin\psi \\ \sin\psi & \cos\psi \end{bmatrix}$$

$$R = \begin{bmatrix} \cos\rho_t & -\sin\rho_t \\ \sin\rho_t & \cos\rho^t \end{bmatrix}$$

$$\Sigma = \begin{bmatrix} \cosh\sigma/2 & i\sinh\sigma/2 \\ -i\sinh\sigma/2 & \cosh\sigma/2 \end{bmatrix}$$

$$\Phi = \begin{bmatrix} \exp(-i\varphi) & 0 \\ 0 & \exp(i\varphi) \end{bmatrix} \quad K = \begin{bmatrix} \exp(-\Delta k/2) & 0 \\ 0 & \exp(\Delta k/2) \end{bmatrix}$$

where ρ_t is the rotation, σ the imaginary part of rotation (equal in magnitude to 'D' at large values of β), 2φ the linear phase retardation, Δk the linear dichroism and χ the attenuation coefficient.

From (3), (4) and (5) it follows

$$\left.\begin{aligned} \rho_t - i\sigma &= n(\beta - \hat{\theta}') \\ \varphi - i\frac{\Delta k}{2} &= \cos^{-1}\left[\frac{\sec^2 n\hat{\theta}'}{\sec^2 n\hat{\theta}}\right]^{\frac{1}{2}} \\ \psi &= \tfrac{1}{2}[(n+1)\beta - \rho_t] \end{aligned}\right\} \qquad (6)$$

$$\chi = n\alpha$$

with

$$\hat{\theta}' = \frac{1}{a}\tan^{-1}\left[\frac{\tan\beta \quad \tan}{\tan\hat{\theta}}\right.$$

There are two cases of special interest:

a) $\beta \gg \gamma$

In this case $\varphi = \frac{\Delta k}{2} \quad 0$

and $$\overset{n}{\rho}_t = \rho_t - i\sigma \approx -\frac{n\hat{\gamma}^2}{2\beta}$$

Hence $$\rho_t = -\frac{n(\gamma^2 - \delta^2)}{2\beta}$$

$$\sigma = -\frac{n\gamma\delta}{\beta}$$

Therefore the linear dichroism of the layers not only results in circular dichroism but also makes a contribution to optical rotation which is opposite in sign to that due to linear birefringence. However this contribution is usually very mall.

b) $\beta \ll \gamma$

In this case

$$J_n \approx \exp(-n\alpha)\begin{bmatrix}\cos n\beta & -\sin n\beta \\ \sin n\beta & \cos n\beta\end{bmatrix}\begin{bmatrix}\exp(-i\hat{\gamma}n) & 0 \\ 0 & \exp(i\hat{\gamma}n)\end{bmatrix}$$

From this it follows that at any point in the medium there are two linear vibrations polarized along the local principal axes of the layer. As one moves along the axis in the direction of light propogation, the two vibrations rotate with the principal axes. The phase retardation and amplitude reduction undergone by these two vibrations are the same as in an untwisted nematic.

However at intermediate values of β one has to use the complete expressions (6). The parameter a which is the imaginary part of optical rotation is difficult to measure directly. It is for this reason that we have measured the parameter D defined earlier. In fact far away from T_N, $|D| \simeq |\sigma|$.

5. Discussion

To calculate D theoretically one can use the following relations (which describe the nature of the emergent light when a right or left circularly polarized beam is incident on the specimen]:

$$\begin{bmatrix} A_1 \\ A_2 \end{bmatrix} = \frac{1}{(2)^{\frac{1}{2}}} J_n \begin{bmatrix} 1 \\ i \end{bmatrix} \quad \text{for right circular light.}$$

$$\begin{bmatrix} B_1 \\ B_2 \end{bmatrix} = \frac{1}{(2)^{\frac{1}{2}}} J_n \begin{bmatrix} 1 \\ -i \end{bmatrix} \quad \text{for left circular light.}$$

Then
$$I_R = |A_1|^2 + |A_2|^2$$
$$I_L = |B_1|^2 + |B_2|^2$$

Figure 5 gives the variation of dichroic power with temperature (or inverse pitch) obtained theoretically for a typical system. The parameters P and $\Delta\mu$ pertaining to CM mixture were the same as used in Chapter I. Further the layer birefringence and layer dichroism were assumed to decrease at the same rate with rise of temperature. The linear dichroism (Δk) was taken to be 0.1 x 10^{-3} at $\beta = 3 \times 10^{-3}$ on the lower temperature side of the nematic point. From the figure 5 one finds that $\mathcal{D}$ exhibits anomalous behaviour, the sign of the dichroism being opposite on either side of the nematic point. This prediction has been confirmed experimentally. The theory also leads to an interesting result regarding the dependence of the dichroic power $\mathcal{D}$ on sample thickness. In table 1, the negative peak values of $\mathcal{D}$ for various sample thicknesses are given. It can be inferred that as the sample thickness is increased, $\mathcal{D}$ increases initially reaching a maximum and than decreases. For the range of sample thickness used in the experiments, calculated $\mathcal{D}$ does

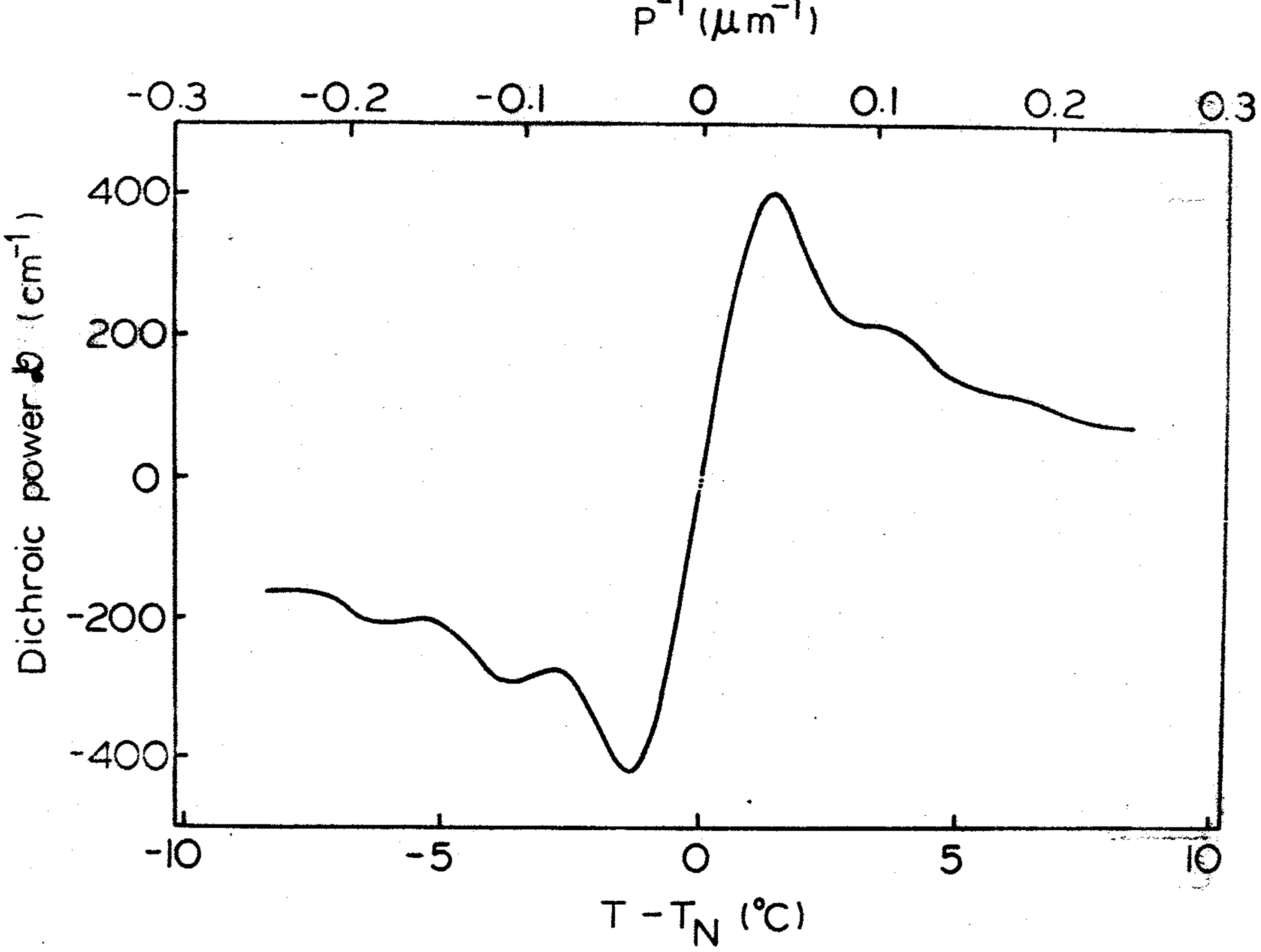
P^{-1} (μm^{-1})
-0.3
-0.2
-0.1
0
0.1
0.2
0.3
Dichroic power $\mathcal{D}$ (cm^{-1})
400
200
0
-200
-400
-10
-5
0
5
10
T − T$_N$ (°C)

Figure 5: Theoretical dependence of dichroic power on temperature and inverse pitch for a 1.75 : 1 CM mixture of sample thickness 6 μm.

Table 1

Sample thickness (in µm)	Negative peak value of ρ
4	430.2
5	441.3
7	366.5
9	348.6
11	341.0
13	305.9

show broadly a decreasing trend with increasing sample thickness, though at a somewhat slower rate than observed experimentally. Considering the uncertainty in the assumed parameters, particularly Δk, it is gratifying that there is, at least, reasonably good qualitative agreement between theory and experiment.

<u>References</u>

Kini, U.D. 1977 Thesis, University of Mysore

Jones, R.C. 1941 J. Opt. Soc. Amer. If, 488.

Ranganath, G.S., Chandrasekhar, S., Kini, U.D., Suresh, K.A. and Ramaseshan, S. 1973 Chem. Phys. Lett. <u>19</u>, 556.

Ranganath, G.S., Suresh, K.A., Rajagopalan, S.R. and Kini U.D. 1973 Proceedings of the International Liquid Crystals Conference, Bangalore (1973) - Pramana Supplement No.1, 353.

Sackmann, E. and Voss, J. 1972 Chem. Phys. Lett. <u>14</u>, 528.

Saeva, F.D. and Wysocki, J.J. 1971 J. Amer. Chem. Soc. , 5928.